Mon. Not. R. Astron. Soc. **000**, 000–000 (0000) Printed 14 March 2016 (MN LATEX style file v2.2)

Suppression of galactic outflows by cosmological infall and circumgalactic medium

Priyanka Singh[1⋆], Sandeep Rana[2], Jasjeet S. Bagla[2], Biman B. Nath[1]
[1] *Raman Research Institute, Sadashiva Nagar, Bangalore, 560080, India*
[2] *Indian Institute of Science Education & Research, Mohali, Mohali*

arXiv:1603.03539v1 [astro-ph.GA] 11 Mar 2016

Accepted, Received; in original form

ABSTRACT

We investigate the relative importance of two galactic outflow suppression mechanisms : a) Cosmological infall of the intergalactic gas onto the galaxy, and b) the existence of a hot circumgalactic medium (CGM). Considering only radial motion, the infall reduces the speed of outflowing gas and even halts the outflow, depending on the mass and redshift of the galaxy. For star forming galaxies there exists an upper mass limit beyond which outflows are suppressed by the gravitational field of the galaxy. We find that infall can reduce this upper mass limit approximately by a factor of two (independent of the redshift). Massive galaxies ($\gtrsim 10^{12} M_{\odot}$) host large reservoir of hot, diffuse CGM around the central part of the galaxy. The CGM acts as a barrier between the infalling and outflowing gas and provides an additional source of outflow suppression. We find that at low redshifts ($z \lesssim 3.5$), the CGM is more effective than the infall in suppressing the outflows. Together, these two processes give a mass range in which galaxies are unable to have effective outflows. We also discuss the impact of outflow suppression on the enrichment history of the galaxy and its environment.

Key words: Galaxies: Haloes; Galaxies: Intergalactic medium

1 INTRODUCTION

The two components of matter in galaxies– dark matter and baryons– have contrasting properties, a fact which makes the study of galactic evolution a complex one. Unlike dark matter, baryons undergo collisions, radiate, and condense towards the central part of the galaxy in order to form stars. However, a significant fraction of these baryons may remain too hot to condense and form stars, especially in large galaxies. This gas likely stays in a hot, diffuse, gaseous form and envelopes the central, optically visible part of the galaxy (Rees & Ostriker 1977; Silk 1977). This gaseous component of the galaxy is referred to as the circumgalactic medium (CGM). Recent observations have indicated the presence of the CGM in massive galaxies (Anderson & Bregman 2011; Dai et al. 2012; Anderson, Bregman & Dai 2013; Bogdán et al. 2013b,a), perhaps extending up to the virial radius of the galaxy.

Galaxies also undergo feedback processes like supernovae (SNe) and active galactic nuclei (AGN) which may give rise to galactic-scale outflows (Croton et al. 2006; Davé, Oppenheimer & Finlator 2011; Vogelsberger et al. 2013). Simultaneously, the galaxies also accrete matter from their surrounding intergalactic medium (IGM) (Birnboim & Dekel 2003; Kereš et al. 2005; Oppenheimer et al. 2010). Together, the infall and outflows regulate the evolution of the host galaxies. However, the interaction between these two opposing processes is not yet well understood.

The CGM can also act as a barrier for infalling gas as well as the outflowing material if the CGM gas cooling timescale is comparable to or larger than the halo destruction timescale (Singh et al. 2015) leading to a hot, diffuse gaseous barrier between the central galaxy and IGM. Recent results of observations (Mathes et al. 2014) and simulations (Goerdt & Ceverino 2015; Gabor & Davé 2015) can be explained by the existence of the hot CGM suppressing the outflows as well as infall. The outflows are generally metal rich and remove a significant amount of metal from galaxies. Since the outflows can be decelerated and even stopped by the hot CGM in massive galaxies, the recycling of metals in massive galaxies becomes more important as compared to the low mass galaxies. This mass dependent recycling behaviour is known as the differential wind recycling (Oppenheimer et al. 2010) and it can alter the metal evolution history of these galaxies and the surrounding IGM. For low mass galaxies($M_h \lesssim 10^{12} M_{\odot}$), the gas cooling timescale is small compared the halo destruction timescale. As a result low mass galaxies cannot sustain the hot CGM gas. This gas cools down, form clumps and does not interfere much with

⋆ priyankas@rri.res.in

in the infall/outflows. Whereas, in case of massive galaxies, the CGM gas remains hot for long enough timescale, leading to the existence of hot, gaseous barrier decelerating infalling (Dekel & Birnboim 2006) as well as outflowing material. Therefore, the presence of the hot CGM divides the galaxies into two categories: 1). Massive galaxies ($M_h \gtrsim 10^{12} M_\odot$), where the CGM is hot enough to affect the physical properties (infall, outflows, metal enrichment etc.) of the galaxy and the wind recycling becomes important, 2). low mass galaxies ($M_h \lesssim 10^{12} M_\odot$), where the CGM cools fast enough and is essentially invisible to the outflowing and infalling gas.

In this work, we address the question of interaction between outflows, infalling gas and CGM from a different perspective. Instead of focussing on the fate of infalling gas, we would like to study the effect of infalling gas and CGM on the outflowing gas. Can outflowing gas escape to the IGM, or is its ultimate mixing with the IGM suppressed? How does this suppression, if at all, depend on the galactic mass and redshift? The possible suppression of outflows is more important for low mass haloes where the hot CGM is essentially absent. For a given halo mass, there exists a redshift where the suppression of outflows by the presence of the hot CGM becomes more important than its suppression by infall. The relative importance of the two wind suppression mechanisms depends on the mass and redshift of the galactic halo. Therefore, it is important to take into account both the mechanisms to understand the galaxy evolution and enrichment.

However, the task is made a difficult one by the complications inherent in the physics of outflowing gas, and also in the complicated nature of infalling gas. Firstly, the outflowing gas may not be spherically symmetric and may have a complicated density, temperature and velocity structure, and this structure itself may be a function of time. Secondly, the infalling gas may also have an anisotropic density and velocity structure. One way to approach the problem is to use cosmological hydrodynamical simulations, which, however, is unlikely to help in understanding the physical processes involved, because of the complexity of the processes. The other approach is to set up idealised numerical experiments, in which certain parameters are varied keeping the others constant, and the processes are studied in detail. However, even before such an exercise, it is useful to study idealised theoretical scenarios with a mix of analytical and numerical tools. This is what we attempt here. In this paper, for outflows, we use the analytical prescription by Sharma & Nath (2013). For infall we use N-body simulations with TreePM code and $N = 512^3$ particles (Bagla 2002; Khandai & Bagla 2009). Used together, they allow us to arrive at a few interesting conclusions regarding the suppression of outflows by infalling matter and CGM, which may have important implications in the cosmological context.

This paper is organized as follows: In section-2 we describe the formalism used to calculate the infall and outflow velocities. In section-3 we discuss the outflow suppression processes and estimate the relative importance of these processes. In section-4 we discuss the impact of the suppression on the IGM enrichment and present our main conclusions in section-6.

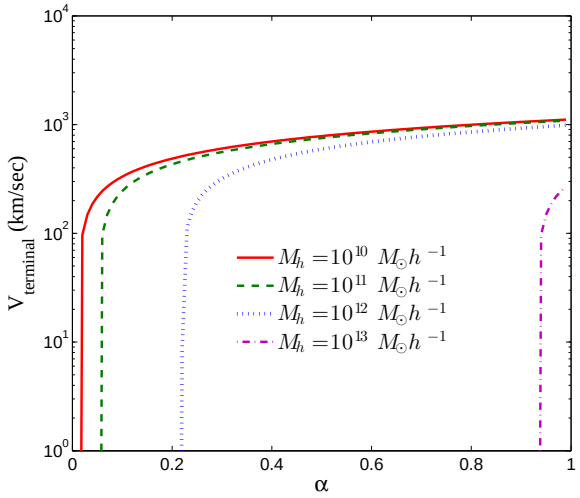

Figure 1. Terminal wind velocity as a function of energy injection efficiency α, due to stellar feedback processes, for galactic haloes in the mass range, $10^{10-13} M_\odot h^{-1}$ (shown in different colors), at redshift, $z = 0$.

2 FORMALISM

2.1 Outflow velocity

The velocity of the outflowing gas mainly depends on the mass and redshift of the galactic halo and the feedback recipe considered. Sharma & Nath (2013) derived the terminal velocity of outflows driven by multiple supernovae in a galaxy whose dark matter profile is described by the Navarro-Frenk-White (NFW) profile. They showed that the wind speed at large galacto-centric distance depends on two velocity scales: (a) v_*, which depends on the mass and energy deposition rate due to supernovae, and is given by $v_* \approx (\dot{E}/2\dot{M})^{1/2}$, and (b) v_s, which depends on the dark matter profile, and is closely related to the circular speed in a NFW profile. The terminal speed of winds (in the absence of momentum injection from active galactic nuclei) was shown to be,

$$v_{\rm wind}(r) = 2\Big[v_*^2 - \frac{1}{2}\Big[\phi_{NFW}(r) - \phi_{NFW}(R)\Big]\Big]^{1/2} \qquad (1)$$

where R=200pc is assumed to be the sonic point, as well as the size of the region in which mass and energy is being injected and $\phi_{NFW}(r) = -2v_s^2 \frac{\ln(1+r/r_s)}{r/r_s}$ is the NFW gravitational potential. The terminal wind velocity ($r \to \infty$) is given by:

$$v_{\rm term} = 2(v_*^2 - v_s^2)^{1/2} \qquad (2)$$

The velocity scale inherent in the energy deposition is given by $v_* = 562\sqrt{\alpha}$ km/s, and it is due to effect of SNe, where α represents energy injection efficiency. The other velocity scale, $v_s = \sqrt{\frac{GM_h}{Cr_s}}$ is due to the gravity of the halo, where, M_h is the virial mass of the halo, $r_s = R_v/c$ is the scale radius of the halo, $C = \ln(1+c) - c/(1+c)$ and $c(M, Z)$ is the concentration parameter (Muñoz-Cuartas et al. 2011).

In Figure-1, we show the terminal wind velocity as a function of α, for the halo mass range $\sim 10^{10}$-$10^{13} h^{-1} M_\odot$, at z=0. For a given halo mass and redshift, the terminal

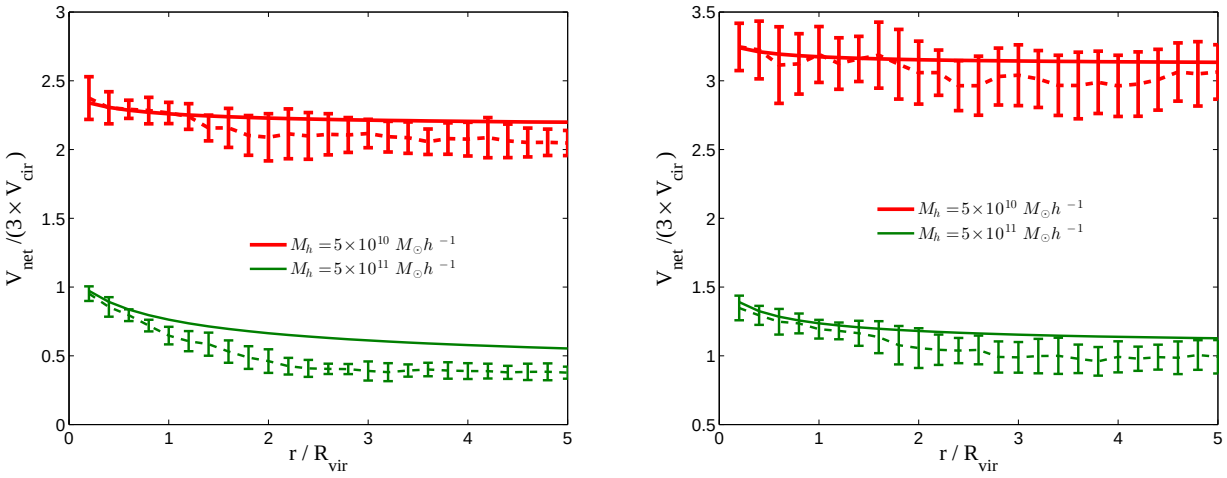

Figure 2. Ratio of outflow velocity to 3×circular speed of the halo as a function of $r/R_{\rm vir}$ at z=3.0 (left panel) and z=1.0 (right panel). The thick red (thin green) solid line represents the unsuppressed wind velocity whereas the dashed line represents the net outflow velocity (wind velocity-infall velocity) for halo mass $M_h = 5 \times 10^{10} M_\odot h^{-1}$ ($M_h = 5 \times 10^{11} M_\odot h^{-1}$) at corresponding redshifts.

wind velocity is close to zero below a particular value of α ($v_* < v_s$), beyond which there is a sharp increase in the wind velocity ($v_* > v_s$) and with further increase in α, the terminal velocity varies slowly ($v_{\rm term} \propto \sqrt{\alpha}$).

Recent hydrodynamical simulations have shown that the efficiency of energy deposition by multiple SNe can be as large as $\approx$ 0.3, which signifies that the rest of the energy is lost in radiation (Sharma et al. 2014; Vasiliev, Nath & Shchekinov 2015). These studies have investigated the radiative energy loss in the case of SNe that are separated in time and in space, but are coherent enough to mildly compensate for the radiative loss. This is also corroborated by inference from X-ray observations of outflows from M82 by Strickland & Heckman (2009). We fix the value of α at 0.3 for the rest of this work.

2.2 Infall velocity

We use gravity only simulations run with the TreePM code (Bagla 2002; Khandai & Bagla 2009) to compute the velocity of infalling gas under the assumption that the gas particles follow the dark matter particles. The suite of simulations used here is described in the Table 1. The cosmological model and the power spectrum of fluctuations corresponds to the best fit model for WMAP-5: $\Omega_{nr} = 0.26$, $\Omega_\Lambda = 0.74$, $n_s = 0.96$, $\sigma_8 = 0.79$, $h = 0.72$, $\Omega_b h^2 = 0.02273$ (Komatsu et al. 2009).

We use the Friends-of-Friends (FOF) (Davis et al. 1985) algorithm with a linking length $l = 0.2$ to identify haloes and construct a halo catalog. Velocity field around each halo is obtained from the same simulations.

The velocity field in the vicinity of haloes is highly anisotropic with infall often along filaments and sheets. We simplify the discussion here by considering only the radial motion around haloes, and also by averaging in all directions around haloes. This is an idealisation but should suffice to give us a glimpse of the relative role of infall and outflows.

In order to calculate the infall speed (and hence the net outflow speed), we divided the region around the halo into shells of thickness $R_{\rm vir}/5$, where $R_{\rm vir}$ is the virial radius of the halo. We calculate the average infall velocity of the shell by averaging over the radial velocity of the particles present in the shell. This gives the infall velocity of each shell as a function of distance from the centre of the halo. We then average this radial infall velocity for approximately ten randomly selected haloes for every mass scale and snapshot. This gives the average radial infall velocity as a function of halo mass and redshift.

Table 1. The table lists the simulations used here. The first column lists the comoving size of the simulation box, the second column lists the minimum halo mass that we can resolve in the simulations, this is given in units of solar mass. Each simulation was run with 512^3 particles. Cosmological parameters used here are described in text.

$L_{\rm box}$ (Mpc)	$M_{\rm min}$ ($M_\odot$)
51.2 h^{-1}	$10^{9.02}$
76.8 h^{-1}	$10^{9.43}$
153.6 h^{-1}	$10^{10.33}$

3 SUPPRESSION OF OUTFLOWS

3.1 Suppression by infall

Subtracting the infall velocity from the radial outflow velocity gives the net outflow velocity. This approach ignores the effect of pressure and assumes a pure advection of outflow in the velocity field. Thus our estimate of the effect of infall on outflows is likely to be an under-estimate.

In Figure- 2, we show the variation of the wind velocity and the net outflow velocity (wind velocity-infall velocity) as a function of the distance from the centre of the dark

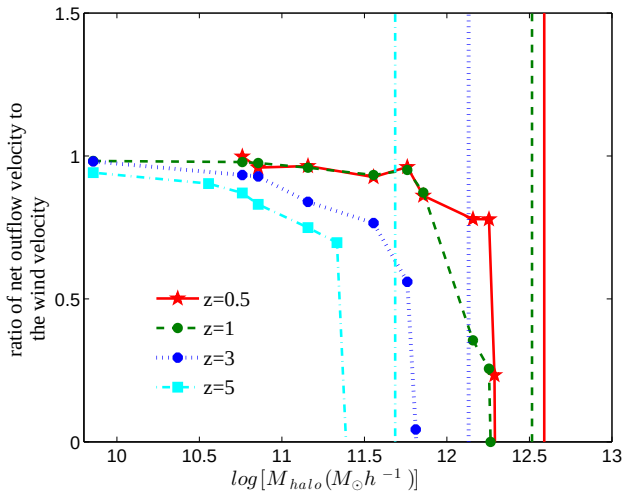

Figure 3. Ratio of net outflow velocity with and without the infall, as a function of the halo mass, for different redshifts (shown in different colors). The vertical lines represent the mass limit above which the outflows cannot overcome the gravitational field of the galaxy and the galaxies do not host the outflows even in the absence of the infall.

matter halo. We plot the ratio of distance from the centre to the virial radius of the halo on the x-axis, and the ratio of net outflow speed to 3×circular speed of the halo along the y-axis. We also show the root-mean-square error on the net outflow velocity. The main features of these plots are as follows:

- For a given redshift, the effect of infall increases with the increasing halo mass. This is mainly due to the increase in the gravitational field of the galaxy with its increasing mass, resulting in higher infall velocity.
- For a given halo mass, the effect of infall increases with the increasing redshift. This behaviour is due to the hierarchical formation history of the universe. Small galaxies form early in the universe at high σ-peaks. These galaxies then grow through accretion and merger to form larger galaxies and galaxy clusters. The same halo mass corresponds to higher σ-peaks resulting in higher infall velocity at higher redshifts.

Thus, by neglecting the effect of infall one may over-predict the outflow velocity and hence the mass outflow rate.

In Figure-3 we show the ratio of the net outflow velocity with and without taking into account the effect of infall. To find this ratio, we calculate the average radial velocity of the shells between $R_{\rm vir}$ and $2R_{\rm vir}$, for different redshifts. For a given mass, the suppression of outflow due to the presence of infall increases with increasing redshift. This effect is more prominent for high mass haloes as compared to low mass haloes. For example, haloes with $M_h \sim 10^{10}h^{-1}M_\odot$, the difference in the suppression of the outflow due to infalling gas is <10% in the redshift range 0.5-5.0, whereas this difference increases to 20% at $M_h \sim 10^{11}h^{-1}M_\odot$ and 50% at $M_h \sim 2\times10^{11}h^{-1}M_\odot$. This variation is due to the decrease in the outflow speed and increase in infall speed with increasing halo mass. This results in the sharp decline in the net outflow speed near $M_{\rm max}$, where $M_{\rm max}$ is the upper mass limit beyond which there are no effective outflows, as predicted by eqn 2. The vertical lines in Figure-(3) show the values of $M_{\rm max}$ at different redshift. The curves in the figure shows that the infall effectively suppresses the outflows even for mass lower than $M_{\rm max}$, effectively decreasing the value of $M_{\rm max}$, beyond which outflows cannot reach the IGM. We find that the value of $M_{\rm max}$ decreases nearly by a factor of 2 due to the presence of infall.

Next, in Figure-4 we show $M_{\rm max}^{\rm infall}$, the upper mass limit beyond which there are no effective outflows as function of redshift. $M_{\rm max}^{\rm infall}$ includes the effect of suppression of outflows due the presence of infall which decreases the value of $M_{\rm max}$ approximately by a factor of two, independent of the redshift, as shown in Figure-3 and to illustrate this effect, we compare $M_{\rm max}$ (thin dashed, brown line) with $M_{\rm max}^{\rm infall}$ as a function of redshift. In this figure, we also show the value of $M_{\rm max}^{\rm infall}$ when the infall velocity is calculated analytically from a spherical top hat model (thin solid, cyan line). It is interesting to find that the prediction of $M_{\rm max}^{\rm infall}$ from N-body simulation (dot-dashed, blue line) and spherical collapse model agree well with each other.

3.2 Suppression by hot CGM

In Figure-4, we also show $M_{\rm max}^{\rm CGM}$ (dotted, pink line), which is the mass limit above which the hot CGM exists in the galactic halo. This mass limit is determined by the condition $\frac{t_{cool}}{t_{dest}} > 1$, where t_{cool} is the halo gas cooling time and t_{dest} is the timescale in which a halo forms a larger halo through merger or accretion and the halo gas is reheated during the process (Singh et al. 2015). The gas cooling timescale is given by $t_{\rm cool} = 3n_pkT/(2n_e^2\Lambda(Z,T))$, where T is the gas temperature (assumed to be the virial temperature of the galaxy), n_e is the electron density (computed assuming that the CGM contains approximately 10% of the total halo mass), $n_p(\sim \mu_e n_e/\mu)$ is the total particle density with μ and μ_e the mean molecular weight of the gas and per free electron respectively and $\Lambda(Z,T)$ is the cooling function (Sutherland & Dopita 1993) which depends on gas temperature and metallicity. The metallicity of the CGM is assumed to be $\sim 0.1Z_\odot$. The value of $M_{\rm max}^{\rm CGM}$ is consistent with earlier studies by Birnboim & Dekel (2003) and Kereš et al. (2005). It changes only slightly with redshift and is comparable to $M_{\rm max}^{\rm infall}$.

Recent simulations have found that for the haloes more massive than $M_{\rm max}^{\rm CGM}$, the outflow speed is reduced to the sound speed in the CGM (Sarkar et al. 2015) due to the presence of hot environment around the central galaxy. This decelerates the outflow and even turns it around to form a galactic fountain.

The observations by Mathes et al. (2014) showed that the fraction of clouds escaping the galactic halo decreases with increasing halo mass. They studied a sample of 14 galaxies in the redshift range $0.1 < z < 0.7$ using the quasar absorption spectroscopy. The authors divided the galaxy sample into two mass bins: massive galaxies with $M_h > 10^{11.5}M_\odot$ and the low mass galaxies with $M_h < 10^{11.5}M_\odot$. The cloud escape fraction (within the virial radius of the galaxy) for the low mass galaxies is $\sim$ 55% whereas the escape fraction decreases significantly to $\sim$ 5% for massive galaxies. It is interesting to find that the dividing mass limit

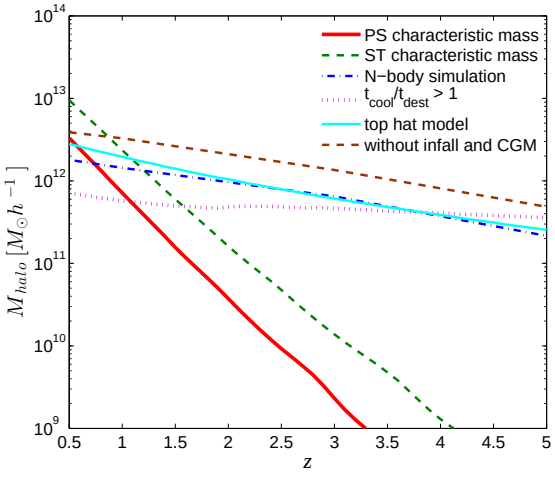

Figure 4. Comparison between $M_{\rm max}$ (thin dashed, brown line) which does not include the suppression of outflows by infall and CGM, $M_{\rm max}^{\rm infall}$ calculated for N-body simulation (dot-dashed, blue line) and the top hat model (thin solid, cyan line), $M_{\rm max}^{\rm CGM}$ (dotted, pink line) and $M_{\rm char}$ calculated for the PS (thick solid, red line) and ST (dashed, green line) mass function.

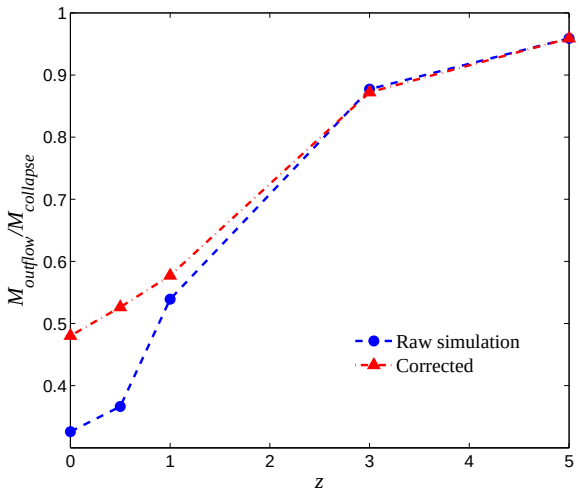

Figure 5. The ratio of mass in haloes hosting unsuppressed outflows to the total mass in all collapsed structures. The blue curve (dashed) shows the ratio as determined in N-Body simulations. Given that we use simulations with different mass resolution and we are unable to resolve low mass haloes in simulations used at low redshifts, this approach under-estimates the ratio. The red curve (dot-dashed) is obtained by applying a correction by extrapolating the mass function to the same mass resolution as is available in the simulations used for high redshift snapshots. The qualitative trend remains the same though the ratio has the value closer to 0.5 rather than 0.3.

between the two samples is comparable to $M_{\rm max}^{\rm CGM}$ determined in the present work. This observation supports the scenario of differential wind recycling where the hot halo gas in massive galaxies decelerates the outflowing clouds. For low mass galaxies $M_h \lesssim 10^{12} M_\odot$, the CGM cooling time is short (compared to halo destruction time), and, consequently, the gas pressure is not sufficient to support against gravity. As a result, the gas forms clumps, reducing its covering fraction and hence the efficiency to suppress outflows.

We note that, in addition to interfering with outflows, hot CGM forms a barrier in front of the infalling gas. In a recent study by Gabor & Davé (2015), the authors found the quenching of star formation due to the suppression of direct supply of the gas to the central galaxy, in the mass range $10^{12} - 10^{13} M_\odot$. The zoom-in hydrodynamic simulations by Goerdt & Ceverino (2015) predict that the gas infall velocity increases with increasing halo mass up to $M_h \approx 10^{12} M_\odot$ beyond which the infall velocity decreases as the halo mass is increased. Note that, the halo mass where the relation between the infall velocity and the halo mass is reversed, is independent of the galaxy redshift and its comparable to $M_{\rm max}^{\rm CGM}$. This indicates that the presence of hot CGM decreases the infall velocity. However, Nelson et al. (2015b) found a significant suppression of the infall by the galactic winds at small r ($< 0.5 R_{\rm vir}$) but they did not find any change in accretion properties as a function of halo mass, in the mass range 10^{10}-$10^{12} M_\odot$. Note that this is still not in disagreement with differential wind recycling scenario if one uses $M_h \sim 10^{12} M_\odot$ as a dividing line between the galaxies with and without a hot circumgalactic environment.

3.3 Relative importance of infall versus hot CGM in suppressing outflows

The cosmological infall and the presence of hot CGM, both give the upper mass limits, $M_{\rm max}^{\rm infall}$ and $M_{\rm max}^{\rm CGM}$ respectively, beyond which the outflow is halted. If $M_{\rm max}^{\rm infall} < M_{\rm max}^{\rm CGM}$, the outflow is suppressed by the infall, even before the existence of the pressure supported, hot circumgalactic gas. In this scenario, the infall plays more important role than the CGM in suppressing the outflows. However, if $M_{\rm max}^{\rm infall} > M_{\rm max}^{\rm CGM}$, the galaxies host the hot CGM before the infall velocity becomes comparable to the outflow velocity. Therefore, the process corresponding to minimum of the two mass-limits, dominants the suppression. Comparing $M_{\rm max}^{\rm infall}$ and $M_{\rm max}^{\rm CGM}$ (see figure-4) suggest that at low redshifts ($z \lesssim 3.5$), the role of hot CGM, in suppressing the outflows is more important than the infall, since $M_{\rm max}^{\rm infall} > M_{\rm max}^{\rm CGM}$, whereas at high redshifts where $M_{\rm max}^{\rm infall} < M_{\rm max}^{\rm CGM} (z > 3.5)$, infall suppresses the outflow more effectively than the CGM. The two mass limits are close in the redshift range considered. $M_{\rm max}^{\rm infall}$ is larger than $M_{\rm max}^{\rm CGM}$ by a factor of $2-3$ near $z \sim 0$. The difference between the two mass-limits decreases with increasing redshift. Therefore, these two processes give a mass range separating the haloes with and without effective outflows.

4 FRACTION OF GALAXIES AFFECTED BY THE SUPPRESSION OF OUTFLOWS

The intergalactic medium is enriched by metals ejected by galaxies through galactic winds. Therefore, the enrichment level of IGM crucially depends on the feedback mechanism, which throws out metals into the IGM and the processes such as infall and the existence of hot CGM, which suppress the outflows. In this section, we examine whether the sup-

pression of outflows by cosmological infall/hot CGM affects a significant fraction of the galaxy population.

In Figure-4, we also show the characteristic mass $M_{\rm char}$ for the Press-Schechter (PS) (defined as $\frac{\delta^2(z)}{2\sigma^2(M_{\rm char})} = 1$) as well as Sheth-Tormen (ST) mass function ($\alpha_{\rm ST}\frac{\delta^2(z)}{2\sigma^2(M_{\rm char})} = 1$, where $\alpha_{\rm ST} = 0.707$). The characteristic mass, $M_{\rm char}$ represents the mass scale beyond which the number of haloes decreases rapidly with increasing halo mass. Therefore, the haloes with masses below $M_{\rm char}$, dominate the halo population. The present day value of $M_{\rm char} \sim 1.4 \times 10^{13} h^{-1} M_{\odot}$ for Press-Schechter mass function and it decreases with increasing redshift as expected from the hierarchical structure formation scenario. We find that at $z > 1-2$, $M_{\rm max}^{\rm infall}$ and $M_{\rm max}^{\rm CGM} > M_{\rm char}$, which implies that the haloes in which outflows are completely suppressed by infalling gas or the presence of the hot CGM, are rare. At low redshifts, majority of the haloes lie near the characteristic mass range, and therefore outflow suppression becomes important. Therefore, the suppression of the outflows due the infall as well as the hot CGM should be taken into account while dealing with the haloes hosting outflows, especially at low redshifts.

Next, to get an estimate of the population of galaxies with suppressed or unsuppressed outflows, we compute the ratio of the total mass in the galaxies hosting unsuppressed outflows to the total mass present in collapsed structures. In Figure-5, we show this ratio as a function of redshift. The total mass in the collapsed structures is estimated using the N-body simulation. To compute the mass in the haloes supporting outflows, we consider haloes with $M_h \lesssim Min[M_{\rm max}^{\rm infall}, M_{\rm max}^{\rm CGM}]$. Note that, while calculating the number of galaxies with unsuppressed outflows, we exclude those haloes in which outflows are *completely* suppressed. Therefore, the ratio includes galaxies with partially suppressed outflows.

Given that the mass resolution of simulations used in this study is different, and that simulations with a larger box-size are required for low redshift studies (Bagla & Prasad 2006), the mass resolution is not independent of redshift in the analysis. The mass resolution is poorer at low redshifts and therefore we miss out on low mass haloes that can potentially contribute to outflows. To overcome this problem, we compute the mass function at each redshift and extrapolate it to the mass resolution of the highest resolution simulation used here. The red curve (dot-dashed) in figure-5 incorporates this correction while computing the ratio of total mass in galaxies that have an unsuppressed outflow to the total mass in collapsed haloes.

The ratio is close to unity at high redshifts ($z \gtrsim 5$) due to the hierarchical formation history of the universe, the haloes at high redshifts are mostly low mass ones. The fraction of mass present in the outflow-supporting haloes decreases with decreasing redshift due to the formation of massive haloes at low redshifts. The redshift range, $z \sim 1-2$, represents the era of high star formation activity. Hence, the abundance of outflow supporting systems can potentially determine the enrichment history of the galaxies, CGM and IGM. We find that the ratio $M_{outflow}/M_{collapse}$ decreases from 70% to 60% in this redshift range. Thus, a small but significant fraction of haloes lie in the mass range where the outflows are completely suppressed by the infall or the presence of the hot CGM during the era of high star formation hence high feedback activity. In the redshift range $z < 1$, $M_{outflow}/M_{collapse}$ decreases from 60% to less than 50%. Since, the presence of the hot CGM is more important at low redshifts (see figure-4), the outflowing gas in approximately half of the haloes at low redshift, is decelerated and suppressed by the surrounding CGM in these galactic haloes.

Therefore, the enrichment of the IGM is easier at high redshifts whereas at low redshifts, the metal carrying outflows are suppressed more effectively, mostly by the hot CGM. These suppressed outflows are then recycled into the galaxy hence enriching the CGM as well as the stars. This result is in agreement with the simulation result of Davé & Oppenheimer (2007), indicating that the IGM contains more metals at high redshifts whereas the stars and the halo gas contain more metals at low redshifts.

5 CAVEATS

The usefulness of our results discussed above is, however, subject to certain caveats. Firstly, the geometry of the infalling gas near the virial radius may not be isotropic as we have assumed, and is likely to be in the form of streams (Dekel, Sari & Ceverino 2009; Dekel et al. 2009). Simulations show that gas mainly flows along filaments in the cosmic web, and the enhanced density of gas in the filaments causes it to cool, and avoids being shocked to the virial temperature (Birnboim & Dekel 2003). Considerations of such cold streams with regard to the fraction of outflowing gas that can escape is difficult without hydrodynamical simulations, and beyond the scope of the present work. However, we note that the cold mode of accretion dominates galaxies below the mass scale of $\sim 10^{12}$ $M_{\odot}$, and the mode of accretion changes to that of slow cooling from hot halo gas (hot mode) beyond this mass scale (Kereš et al. 2005). The shock heating and disruption of cold infalling streams, especially at high redshifts and low galacto-centric radii, becomes more important near $M_h \sim 10^{12}$ $M_{\odot}$ (Danovich et al. 2012; Nelson et al. 2013; Danovich et al. 2015; Gabor & Bournaud 2014; Nelson et al. 2015a). This mass scale coincides with the mass scale shown in Figure-4 (dotted pink line corresponding to the galactic haloes with $t_{\rm cool}/t_{\rm dest} > 1$), and therefore the filamentary nature of cold flows in low mass galaxies does not significantly alter our conclusions.

Secondly, all of the CGM gas may not be in a hot, diffuse state, and a fraction of it is likely to be in a warm ($\sim 10^4$ K) phase, as indicated by the COS-Halos survey (Werk et al. 2014). It is also believed that the interaction of the CGM gas with the outflows driven by first phases of star formation may cause clumping (Marinacci et al. 2010; Sharma et al. 2014). The gas in the interaction zone may suffer from various instabilities, such as thermal instability (due to the mixing of gas at different temperatures and densities) and Kelvin-Helmholz instability (due to shear). The resulting structures and turbulence in the CGM may allow some fraction of the outflowing gas to escape, in the cases where our results above for a homogeneous CGM may not allow any escape. However, this fraction is difficult to estimate without the aid of hydrodynamic simulations.

However, given these uncertainties, it is interesting to note the similarities of the mass scale we have dis-

cussed so far, that of $M_{\rm max}^{\rm infall}$, with other mass scales that are significant for galaxy evolution. Several studies (e.g, Behroozi, Wechsler & Conroy (2013)) have shown that the ratio of baryonic mass to the total mass of galaxies reaches a maximum around $\sim 10^{12}$ M$_\odot$ at the present epoch, and slightly lower at high redshift (e.g., lower by a factor of ~ 3 at $z \sim 4$). This is remarkably close to the mass scale $M_{\rm max}^{\rm infall}$ shown in Figure-4 (dot-dashed blue line and thin solid cyan line). We can speculate, on the basis of our calculations here, that the stoppage of the outflow is causally connected to the baryon-to-total mass ratio. The analytic work of Sharma et al. (2014), which did not consider the effect of infall or the presence of CGM, and only considered the effect of gravity, has already suggested that the stoppage of outflow is related to the baryons-to-total mass ratio. Our work on the effect of infall and CGM's presence provides additional supports for this scenario.

6 CONCLUSIONS

In this work, we have studied the relative importance of galactic outflows, cosmological infall and the role of presence of hot circumgalactic gas on these processes under some simplified assumptions such as spherically symmetric infall, constant value of energy injection efficiency, and gas particles following the dark matter particles. We have also neglected the complexities involved in the dynamics and distribution of the CGM as well as the infalling gas. However, as discussed in section-5, the detailed treatment of these complexities is unlikely to change the conclusions drawn from our analysis substantially. Our conclusions can be summarised as follows:

(i) Without considering the CGM, the infalling gas interferes with the outflowing gas reducing the net outflow velocity. This reduction depends on the mass and redshift of the galaxy. The larger (massive) galaxies at high redshifts suffer more suppression compared to smaller (low mass) galaxies at low redshifts due to the combined effect of weaker outflows and stronger infall in the case of massive galaxies.

(ii) Even in the absence of any infall, there exits an upper mass limit beyond which the outflows are unable to overcome the gravitational field of the galaxy. This upper mass limit decreases roughly by a factor of two due to the additional suppression of outflows by infalling gas, independent of the redshift. The value of this upper mass limit, $M_{\rm max}^{\rm infall}$, predicted by simulations agrees well with the value predicted by the top-hat model.

(iii) In addition to the infall, the presence of the hot gaseous environment in the form of CGM, decelerates the outflows. The CGM also gives an upper mass limit, $M_{\rm max}^{\rm CGM}$, beyond which the hot CGM effectively stops the outflows from escaping the galaxy. The hot CGM may also reduce the direct supply of infalling gas to the central part of the galaxy. We estimate $M_{\rm max}^{\rm CGM}$ under the condition that the gas cooling time exceeds the halo destruction timescale. $M_{\rm max}^{\rm CGM}$ varies slowly with the redshift with its value $\sim 10^{12} M_\odot$ in the redshift range $0-5$.

(iv) The hot CGM is more effective than the infall in the low redshift range 0-3.5 in counteracting the outflows whereas the infall becomes more effective at high redshift ($z > 3.5$). The upper mass limits, for suppressing the outflows, predicted by both the processes are comparable and together determine the fate of the outflowing gas.

(v) Comparison of $M_{\rm max}^{\rm CGM}$ and $M_{\rm max}^{\rm infall}$ with the characteristic mass predicts the suppression of the outflows to be important at low redshifts ($z < 1-2$), where the galaxies with completely suppressed outflows constitute a significant fraction of the overall galaxy population. The fraction of galaxies with unsuppressed outflows predicted by the simulation decreases from $\sim$90% at $z = 5$ to $\sim$50% at $z = 0$. This fraction is of order 60-70% in the era of high star formation and hence high feedback activity ($z \sim 1-2$), likely affecting the enrichment history of the universe.

ACKNOWLEDGEMENTS

We thank the anonymous referee for valuable comments and suggestions which helped in improving this paper. We also thank Girish Kulkarni and Kartick C. Sarkar for helpfull discussions. PS acknowledges the hospitality of IISER, Mohali.

REFERENCES

Anderson M. E., Bregman J. N., 2011, ApJ, 737, 22
Anderson M. E., Bregman J. N., Dai X., 2013, ApJ, 762, 106
Bagla J. S., 2002, Journal of Astrophysics and Astronomy, 23, 185
Bagla J. S., Prasad J., 2006, MNRAS, 370, 993
Behroozi P. S., Wechsler R. H., Conroy C., 2013, ApJ, 770, 57
Birnboim Y., Dekel A., 2003, MNRAS, 345, 349
Bogdán Á., Forman W. R., Kraft R. P., Jones C., 2013a, ApJ, 772, 98
Bogdán Á. et al., 2013b, ApJ, 772, 97
Croton D. J. et al., 2006, MNRAS, 365, 11
Dai X., Anderson M. E., Bregman J. N., Miller J. M., 2012, ApJ, 755, 107
Danovich M., Dekel A., Hahn O., Ceverino D., Primack J., 2015, MNRAS, 449, 2087
Danovich M., Dekel A., Hahn O., Teyssier R., 2012, MNRAS, 422, 1732
Davé R., Oppenheimer B. D., 2007, MNRAS, 374, 427
Davé R., Oppenheimer B. D., Finlator K., 2011, MNRAS, 415, 11
Davis M., Efstathiou G., Frenk C. S., White S. D. M., 1985, ApJ, 292, 371
Dekel A., Birnboim Y., 2006, MNRAS, 368, 2
Dekel A. et al., 2009, Nature, 457, 451
Dekel A., Sari R., Ceverino D., 2009, ApJ, 703, 785
Gabor J. M., Bournaud F., 2014, MNRAS, 437, L56
Gabor J. M., Davé R., 2015, MNRAS, 447, 374
Goerdt T., Ceverino D., 2015, MNRAS, 450, 3359
Kereš D., Katz N., Weinberg D. H., Davé R., 2005, MNRAS, 363, 2
Khandai N., Bagla J. S., 2009, Research in Astronomy and Astrophysics, 9, 861
Komatsu E. et al., 2009, ApJS, 180, 330
Marinacci F., Binney J., Fraternali F., Nipoti C., Ciotti L., Londrillo P., 2010, MNRAS, 404, 1464
Mathes N. L., Churchill C. W., Kacprzak G. G., Nielsen N. M., Trujillo-Gomez S., Charlton J., Muzahid S., 2014, ApJ, 792, 128
Muñoz-Cuartas J. C., Macciò A. V., Gottlöber S., Dutton A. A., 2011, MNRAS, 411, 584

Nelson D., Genel S., Pillepich A., Vogelsberger M., Springel V., Hernquist L., 2015a, arXiv:1503.02665
Nelson D., Genel S., Vogelsberger M., Springel V., Sijacki D., Torrey P., Hernquist L., 2015b, MNRAS, 448, 59
Nelson D., Vogelsberger M., Genel S., Sijacki D., Kereš D., Springel V., Hernquist L., 2013, MNRAS, 429, 3353
Oppenheimer B. D., Davé R., Kereš D., Fardal M., Katz N., Kollmeier J. A., Weinberg D. H., 2010, MNRAS, 406, 2325
Rees M. J., Ostriker J. P., 1977, MNRAS, 179, 541
Sarkar K. C., Nath B. B., Sharma P., Shchekinov Y., 2015, MNRAS, 448, 328
Sharma M., Nath B. B., 2013, ApJ, 763, 17
Sharma P., Roy A., Nath B. B., Shchekinov Y., 2014, MNRAS, 443, 3463
Silk J., 1977, ApJ, 211, 638
Singh P., Nath B. B., Majumdar S., Silk J., 2015, MNRAS, 448, 2384
Strickland D. K., Heckman T. M., 2009, ApJ, 697, 2030
Sutherland R. S., Dopita M. A., 1993, ApJS, 88, 253
Vasiliev E. O., Nath B. B., Shchekinov Y., 2015, MNRAS, 446, 1703
Vogelsberger M., Genel S., Sijacki D., Torrey P., Springel V., Hernquist L., 2013, MNRAS, 436, 3031
Werk J. K. et al., 2014, ApJ, 792, 8